



**Learner
Support
Services**

The University of Bradford Institutional Repository

This work is made available online in accordance with publisher policies. Please refer to the repository record for this item and our Policy Document available from the repository home page for further information.

To see the final version of this work please visit the publisher's website. Where available, access to the published online version may require a subscription.

Author(s): Benkreira, H.

Title: Step-change in Enhancing Extrusion as a Unit Operation

Publication year: 2005

Publication: Proceedings of the 7th World Congress of Chemical Engineering

Publisher: IChemE

Publisher's site: <http://www.icheme.org/books>

Copyright statement: © 2005 IChemE. Reproduced in accordance with the publisher's self-archiving policy.

STEP-CHANGE IN ENHANCING EXTRUSION AS A UNIT OPERATION

H.Benkreira (CEng, FIChemE)

School of Engineering, Design & Technology

University of Bradford, Bradford BD7 1DP, email: H.Benkreira@bradford.ac.uk

INTRODUCTION

Extrusion-a unit operation in polymer processing has been in extensive use since the great age of plastic technology. It is a simple operation that enables within one equipment the sequential conveying of solid polymer chips or powder, their melting, mixing, pumping and shaping via a die into a variety of high tonnage and/or value products. Pipes, bottles, films are the most common examples but the list of applications is endless from tiny micromoulded parts to large structural profiles. Extrusion is not limited to plastics but is used hot or cold to process soft solids like food, industrial and pharmaceutical pastes, as well as metals and ceramics. Most of the advances in extrusion processing have concentrated in improving the essential functions of extrusion: solid conveying, melting, pumping and mixing. The literature abounds with descriptions of such advances pushing the limits of the extrusion in an *incremental* way. In this paper, we describe *step-changes* in enhancing extrusion, which opens up new applications to better old technology-make them safer, cheaper and cleaner. The new designs presented in this paper have also the potential to develop new reactor technology for viscous fluids.

THE ROLLER DIE EXTRUDER

Principle of Operation

To date all extruder dies have been *stationary*. The step-change in our new designs is to juxtapose to the extruder a *moving* die, which will affect flow other than by just its geometry (Figure 1). In other words die gap-where the melt flows out of the extruder is not the only flow control variables. In the roller die design, die-dynamics are additional flow control variables.

In our design, the moving die consists of two rotating rollers, which can oppose or drag the extrusion flow. In the forward mode, the rollers drag the extrudate out at low pressures and the output rate is increased. This mode of operation can be exploited to extrude "normal" viscosity materials at lower temperatures. In the counter-flow mode, very large pressure can be developed in the die without having to reduce the gap. [Remember in a sheet die (or tube die assumed to be a sheet wrapped into a circle) pressure drop is related to thickness H^3]. High-pressure (>100bars) extrusion without sheet thickness reduction opens up new opportunities for developing new

processing routes. One example is in the production of low-density thick plastic foams. Rather than using the environmentally damaging hydrochlorofluorocarbons (HCFC), supercritical CO₂ instead can be used as the foam-blowing agent. Also, supercritical CO₂ is known as a plasticiser even in very small proportion (1%) and its addition to polymers enables their processing at lower temperatures. This is useful particularly with recycled plastics, which have a tendency to degrade at normal extrusion temperature. Any reduction in processing temperature in this application will enhance processing and encourage recycling.

The roller die concept can be extended further by juxtaposing pair of rollers. When two pairs of rollers, one pair rotating backward followed by one pair rotating forward, are used, pressure is increased and pressure drop is accelerated. This operating mode is new and can be used to control co-extrusion. Layer thickness can be controlled from screw speed, or more possibly, by gear pumps. The latter are very expensive and unsuitable for some materials. Pairs of rollers could be used to control flow rate (running backward or forwards) and might be profiled to change the influence between centre and edges.

Theoretical Underpinning

Having developed the concept, it is desirable to provide a theoretical underpinning to guide design and operation. As is done in classical extrusion, the flow model consists of the extruder-die-land in series. The only difference here is the die consists of a set of moving rollers (Figure 2). We illustrate the approach to the backward and forward mode noting that the same approach can be extended to the combined backward + forward flow. In the backward flow, the key parameter is the pressure P_2 , which dictates in the plastic foam application the amount of CO₂ that can be dissolved in the melt. The larger the P_2 , the lower the foam density. In the forward flow, the application is not in the production of foams so enhancing flow rate Q not P_2 will usually be aim. Illustrating the application to Newtonian melts first, we have the usual lubrication approximation equation for the pressure distribution in the nip between two rollers of equal radius and speed rotating in the same or opposite direction (+/-U):

$$\frac{d\phi}{dx} = 12 \mu \left[\frac{U}{h_R^2} - \frac{Q_R}{h_R^3} \right] \quad (1)$$

The gap is related to flow direction position x and roller radius simply as:

$$h_R = h_{R,0} + R - \sqrt{R^2 - x^2} \quad (2)$$

The pressure distribution equation can thus be integrated to give Q_R in relation to pressure drop $P_3 - P_2$ which develops through length $L_R = x_3 - x_2$:

$$\frac{P_3 - P_2}{L_R} = 12 \mu \left[U \frac{1}{L_R} \int_{x_2}^{x_3} \frac{dx}{h_R^2(x)} - Q_R \frac{1}{L_R} \int_{x_2}^{x_3} \frac{dx}{h_R^3(x)} \right] \quad \text{or}$$

$$Q_R = U \frac{\alpha}{\beta} - \frac{1}{12 \mu \Delta x \beta} (P_3 - P_2) \quad (3)$$

α and β are the integral terms in Eq. 3 and can be evaluated from the geometry of the roller system.

The extruder flow rate Q_E per unit width W_E is related to extruder pressure drop $P_2 - P_1$ by:

$$Q_E = H_E \frac{\pi D N \cos \theta}{2} F_D - \frac{H_E^3}{12 \mu L_E} (P_2 - P_1) F_P \quad (4)$$

H_E is the channel depth, θ the helix angle, D the screw diameter, N the screw speed and L_E the helical length. F_D and F_P are the shape factors for the extrusion drag and pressure flow respectively. Their values, less than 1, depend only on the value of H_E/W_E and can be found in extrusion flow analysis books.

If we juxtapose to the extruder and roller a land section of gap H_L and length L_L as shown in Figure 2, then an additional pressure drop $P_4 - P_3$ occurs and the corresponding land flow rate Q_L per unit width is:

$$Q_L = \frac{H_L^3}{12 \mu L_L} (P_4 - P_3) \quad (5)$$

Mass balance requires that $Q_E = Q_R = Q_L = Q$. Also the pressure drops must sum up to zero or $(P_2 - P_1) - (P_3 - P_2) - (P_4 - P_3) = 0$. The above equations are the design/operation flow equations. They were solved to yield values of P_2 for a required flow rate Q as a function of operating conditions (screw speed, roller speed and gap, extruder, roller die and land geometries and melt viscosity). These operating variables were then manipulated to optimise P_2 for a required flow rate Q and exit gap $h_{R,O}$. To close the model and enable it to predict the foam density in the backward flow, we bring in solubility data [1] of CO_2 in polymer melts and express the mass fraction of CO_2 dissolved as a function of P_2 using Henry's Law or:

$$m_{\text{CO}_2} = \Psi P_2 \quad (6)$$

Upon exiting the extruder, this m_{CO_2} expands into the melt without escaping. Knowing the CO_2 and polymer densities ρ_{CO_2} and ρ_{polym} at atmospheric conditions, we can then calculate the foam density as:

$$\rho_{\text{foam}} = (1 + \Psi P_2) / [(1 / \rho_{\text{polym}}) + (\Psi P_2 / \rho_{\text{CO}_2})] \quad (7)$$

The above analysis is simplified since it assumes isothermal, Newtonian, lubrication type flow. To account for the non-Newtonian shear thinning character of the melt, we have used the power law model modified to account for finite apparent viscosity at low and zero shear rate. In the

calculations, the limiting lower viscosity was taken above and below the critical shear rates where the melt remain essentially Newtonian as showed in the actual rheological data.

Temperature rises due to viscous heating and deviations from one-dimensional flow are more difficult to handle analytically. There are strong circulating flow regions in the backward flow; the lubrication approximations do not hold and both elastic and shear thinning as well as edge effects should be considered. CFD software Fluent PolyFlow with shear heating taken into account was used to simulate 2D (1200 nodes mesh) and 3D (5300 nodes mesh) models of the die. A temperature dependent Carreau-Yasuda Law shear model was used. The simulations were used to arrive at an optimum design.

Experimental Realisation of the Concept

A diagram of the experimental set-up is shown below to illustrate the application to foam production using supercritical CO₂ and the plasticising effect of CO₂. The set-up consists of a single screw extruder, mixing head and roller die attached in series. The CO₂ was injected just prior to the mixing section.

The Extruders- 2 instrumented extruders were used: a 32 mm and a 50 mm with L/D ratios of 20:1 and 25:1. The 50-mm screw has a compression ratio of 3:1. To ensure good mixing a cavity transfer and a static mixer were inserted between the extruder and the roller die, immediately after the CO₂ injection point.

The Roller Dies-They were built with rollers 35-mm long, one of fixed diameter 23-mm and the second with variable diameter so when encased in the frame they produced gaps of 0.5, 0.75, 1, 1.25, 1.5 and 4 mm. The rollers were linked by spur gears and driven at the same speed.

Liquid CO₂ Pump and Injector-Liquid CO₂ was fed from a cylinder via a variable stroke/volume high-pressure pump suitably calibrated and a spring driven valve injector.

Capillary Die- In order to measure the plasticising effect of CO₂ an in-line method was necessary. CO₂-polymer rheology was measured with a 130-mm long 3-mm diameter capillary die inserted in the 50-mm extruder and fitted with pressure probes.

Experimental Programme- 6 polymers were used: LDPE, LLDPE, 2 PS and 2 PP. The shear and extensional viscosities of the melts were measured using a Rosand capillary viscometer with a long and a short capillaries and a Bohlin cone and plate viscometer over a wide range of shear rates (0.1-20,000 s⁻¹) and temperatures (185-225 °C). Polymers were run first without CO₂ to establish the flow and pressure conditions and compared them with model predictions. Conditions that produce high-pressures (up to 3000 psi) were then used to produce polymer foams with injected CO₂. Hydrocerol was used as the nucleating agent. During the foam experiments, the control of pressure was critically dependent on the melt temperature at the die. The experiments were run at

roller gaps of 0.5, 0.75, 1, 1.25, 1.5 and 4 mm in the range of extruder screw speeds. Pressure and temperature data was collected using transducers linked to a PC via an interface and DASYlab software. Output rate was measured by weighting extrudate in a set time. Foam density was measured using a water column. Samples were then microtomed to expose under the microscope the cellular structure, which was measured using pc based image analysis software. To assess circulation in the die, flow visualisations were carried out in a transparent roller die using a CCD camera linked to a PC.

Experimental Data & their Comparison with Predictions

For illustration to plastic foam processing, comparisons were made between the predicted and measured melt pressures and foam densities with the polymers tested. When the analytical model is compared with the experimental data, it generally shows a good fit. The results are of a similar order of magnitude and follow the same trend. There are however discrepancies, particularly with the reverse mode, which clearly violates the lubrication approximation at the extruder-rollers junction where strong 2D flow and recirculation will prevail. As shown in Figure 3, full CFD simulations with shear heating and non-Newtonian rheology taken into account narrow the discrepancy between theory and data. To demonstrate the plasticising effect of CO₂ on polymers, Figure 4 displays the rheological data of the neat polymer melts and the polymer-CO₂ systems. The reduction of viscosity is evident and this will indeed allow processing at lower temperatures.

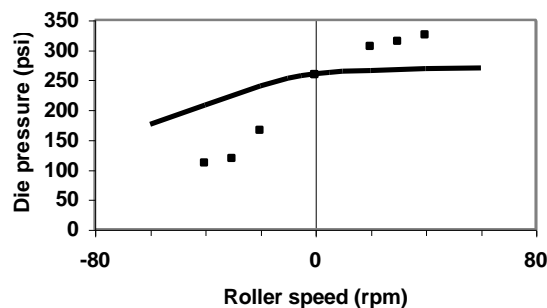


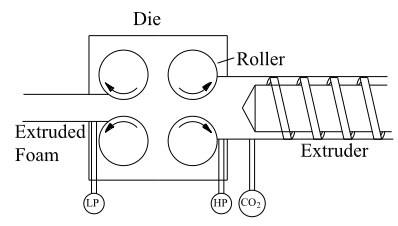
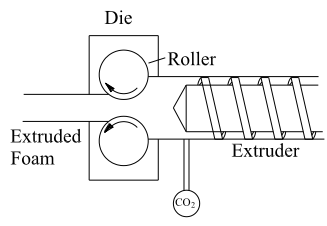
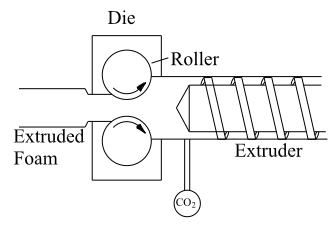
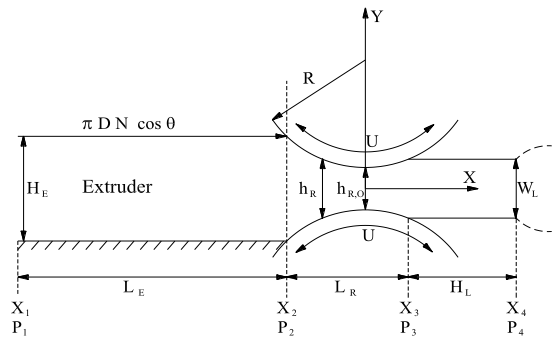
Figure 6 - Comparison of Die Pressures obtained from Experiments and 3D CFD Simulations for PS at 190°C at 15 rpm Screw Speeds and 1.0 mm Die Gap. — Simulations, ■ Data.

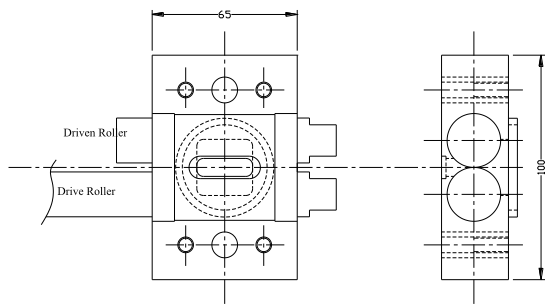
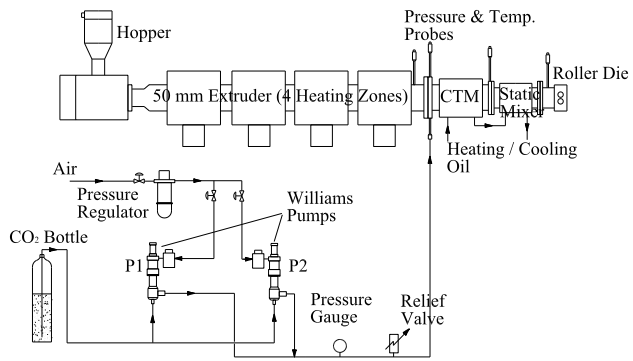
References

1. E. Boy *Non-polluting foaming*, *Kunststoffe Plast Europe*, **87**, 12-13 (1997).
2. F. J. Dietzen *CO₂ as a Blowing Agent for Foamed Polystyrene Sheets*, *Kunststoffe-Plast Europe*, **84**, 565-& (1994).
3. N. Faridi, S. K. Dey and A. Chawda In *Annual Technical Conference - ANTEC, Conference Proceedings*, Vol. 2 Soc of Plastics Engineers, pp. 2221-2226 (1997).
4. H. Benkreira, M. Cox, J. Paragreen and R. Patel *Polymer Processing Society 18*, Guimaraes, Portugal (2002).
5. C. Rauwendaal *Polymer Extrusion*, Hanser Publishers, Munich (1990).
6. Zatloukal M, Vlcek J, Tzoganakis C, Saha P *Journal of non-Newtonian fluid mechanics*, vol 107, pg 13, (2002)
7. A. V. Shenoy and D. R. Saini *Thermoplastic Melt Rheology and Processing*, Marcel Dekker, Inc., New York (1996).
8. Public final report of ESPRIT HPCN PST Activity. *FOAM – HPCN simulation of foam extrusion*. March (1999).
9. Park CB, Behravesh AH, Venter RD, *Polymer Engineering and Science*, vol 38 11 1812-1823 (1998)
Xiang X, Park CB, Donglai X, Pop-Iliev R, *Blowing Agents and Foaming Processes*, Heidelberg, Germany (2002).

References

1. D. Klempner and K. C. Frisch *Handbook of Polymer Foams and Foam Technology*, Hanser Publishers (1991).
2. I. Uniroyal Chemical Company In *Uniroyal Chemical Company, Inc, Product Bulletin* (1992).
3. F. H. Collin *SPE 16th Annual Technical Conference*, (1960).
4. W. A. Jacobs and F. H. Collins *Method of Extruding a Foamed Thermoplastic Product*, United States Patent 3,151,192, (1961).
5. F. A. Carlson *Process of Making Foamed Resins*, United States Patent 2,797,443, (1954).
6. S. T. Lee *Foam Extrusion, Principles and Practice*, Technomic Publishing Company Inc, Pennsylvania, USA, Lancaster USA (2000).
7. D. K. Taylor, R. Carbonell and J. M. DeSimone *OPPORTUNITIES FOR POLLUTION PREVENTION AND ENERGY EFFICIENCY ENABLED BY THE CARBON DIOXIDE TECHNOLOGY PLATFORM*, *Annu. Rev. Energy Environ.*, **25**, 115-146 (2000).
8. R. G. Griskey *SPE Annu Tech Conf, 34th, Proc*, Atlantic City, NJ (1976).
9. N. Faridi, S. K. Dey and A. Chawda In *Annual Technical Conference - ANTEC, Conference Proceedings*, Vol. 2 Soc of Plastics Engineers, pp. 2221-2226 (1997).





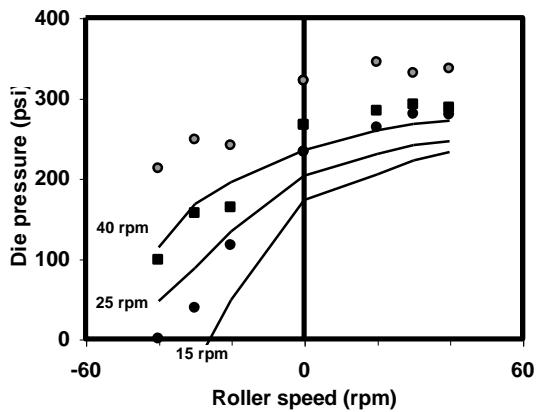


Fig 4.3.4: Comparison of Experimental Pressure data with and the Lubrication Approximation Predictions for PS at 220 °C, Die Gap of 1.0 mm and Screw Speeds of 15 rpm 25 rpm 40 rpm — Lubrication Approximation.

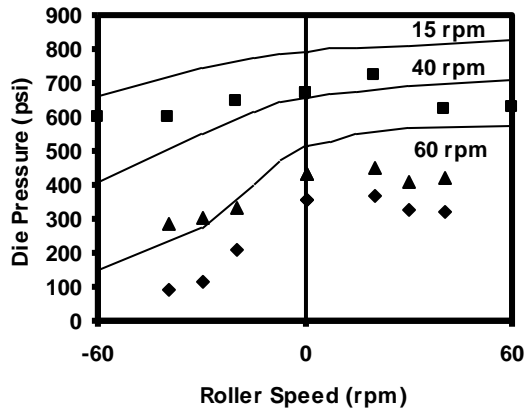


Fig. 4.3.5: Comparison of Die Pressures obtained from Experiments and — CFD Simulations for PS at 220 °C at 15 rpm 40 rpm 60 rpm Screw Speeds and 1.0 mm Die Gap.

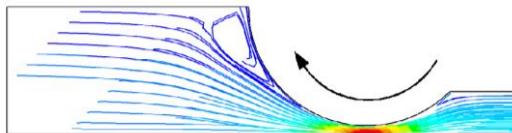


Fig. 4.3.6: CFD Simulations showing Recirculating Flow at a Reverse Roller Speed of 7 rpm, Throughput of 2 kg/hr and 4 mm Die Gap with PS at 200 °C.

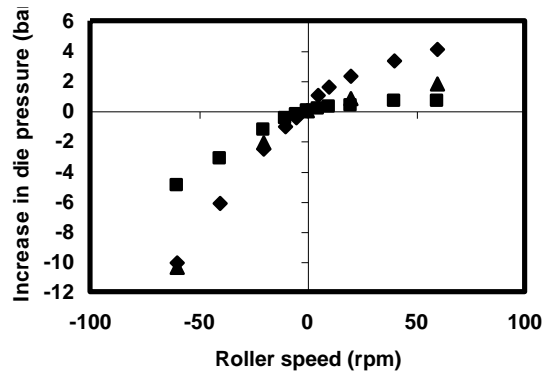


Fig. 4.3.7: Optimisation of roller die width for PS at 190 °C at 15 rpm Screw Speeds and 1.0 mm Die Gap at widths of infinity 5mm and 25mm. Showing rollers at most effective for maximum possible width.

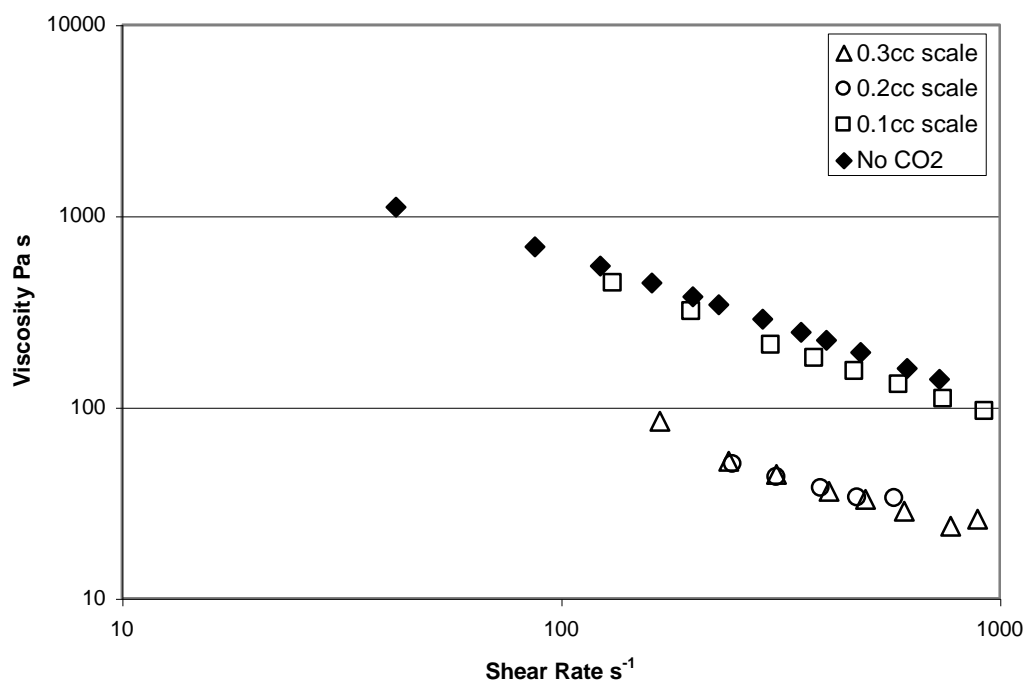


Fig 7 – Effect of CO₂ on melt viscosity at 225°C

